

Identifying the epileptogenic zone by four non-invasive imaging techniques versus stereo-EEG in MRI-negative pre-surgery epilepsy patients



Davide Rossi Sebastiano^{a,*}, Laura Tassi^b, Dunja Duran^c, Elisa Visani^c, Francesca Gozzo^b, Francesco Cardinale^b, Lino Nobili^d, Angelo Del Sole^e, Annalisa Rubino^b, Sara Dotta^a, Elena Schiaffi^a, Rita Garbelli^c, Silvana Franceschetti^c, Roberto Spreafico^c, Ferruccio Panzica^c

^a Neurophysiology Unit, Fondazione IRCCS Istituto Neurologico Carlo Besta, Milan, Italy

^b “Claudio Munari” Epilepsy Surgery Centre, Niguarda Hospital, Milan, Italy

^c Epilepsy Unit, Fondazione IRCCS Istituto Neurologico Carlo Besta, Milan, Italy

^d DINOGMI, University of Genoa, and Child Neuropsychiatry Unit, IRCCS Istituto G. Gaslini, Genoa, Italy

^e Department of Health Sciences, University of Milan and ASST Santi Paolo e Carlo, Milan, Italy

ARTICLE INFO

Article history:

Accepted 22 May 2020

Available online 3 June 2020

Keywords:

MEG
EEG-fMRI
HR-EEG
PET
Epilepsy surgery

HIGHLIGHTS

- Non-invasive techniques considered together reached an accuracy of 60–80% in identifying the epileptogenic zone (EZ) compared to SEEG.
- The diagnostic yield of non-invasive techniques increased in the subgroup of patients with EZ involving two or more lobes.
- EEG-fMRI, MEG or HR-EEG and PET appeared the best combination of techniques in the evaluation of multilobar EZ.

ABSTRACT

Objective: We evaluated four imaging techniques, i.e. Electroencephalography (EEG)-functional Magnetic Resonance Imaging (MRI) (EEG-fMRI), High-resolution EEG (HR-EEG), Magnetoencephalography (MEG) and 2-[18F]fluoro-2-deoxy-D-glucose positron emission tomography (PET), for the identification of the epileptogenic zone (EZ) in 41 patients with negative MRI, candidate to neurosurgery.

Methods: For each technique, results were compared to the Stereo-EEG. Diagnostic measures were calculated with respect to the post-surgical outcome, either for all the patients (39/41, two patients excluded) and for the subgroup of patients with the EZ involving more than one lobe (20/41).

Results: When considered individually, each functional technique showed accuracy values ranging 54,6%–63,2%, having PET, MEG and HR-EEG higher sensitivity, and EEG-fMRI higher specificity. In patients with multilobar epileptogenic zone, functional techniques achieved the best accuracies (up to 80%) when three techniques, including EEG-fMRI, were considered together.

Conclusions: The study highlights the accuracy of a combination of functional imaging techniques in the identification of EZ in MRI negative focal epilepsy. The best diagnostic yield was obtained if the combination of PET, MEG (or HR-EEG as alternative), EEG-fMRI were considered together.

Significance: The functional imaging techniques may improve the presurgical workup of MRI negative focal epilepsy, if epileptogenic zone involves more than one lobe.

© 2020 International Federation of Clinical Neurophysiology. Published by Elsevier B.V. All rights reserved.

1. Introduction

In patients with drug-resistant focal epilepsies, the Epileptogenic Zone (EZ) identification is the main issue to be solved to pro-

* Corresponding author.

E-mail address: davide.rossi@istituto-besta.it (D. Rossi Sebastiano).

pose epilepsy surgery. In most candidates, routine electro-clinical investigations and imaging studies are adequate to identify EZ, with good seizure outcome after surgery. When discrepancies are present and/or when Magnetic Resonance Imaging (MRI) is unrevealing, monitoring by means of invasive Electroencephalography (EEG) is required although seizures relapses are frequent (up to 40% of the patients), not achieving seizure freedom, regardless age, gender and localization of EZ (Télliez-Zenteno et al., 2005). In these cases, the successful surgical treatment remains challenging. Despite the risk (1–4%) of complications (Burneo et al., 2006; Tanrivedi et al., 2009) and the high cost of the procedure (Marras et al., 2013; Picot et al., 2016), the invasive pre-surgical monitoring is still considered the gold standard for the localization of the EZ.

MRI is considered mandatory because of its role in detecting epileptogenic lesions (Wellmer et al., 2013); however, MRI-negative cases still represent 20–40% of surgical candidates (Bien et al., 2009). The unrevealing MRI is one of the main reasons to address patients to invasive pre-surgical monitoring.

Non-invasive functional neuroimaging techniques (NIFNTs), such as 2-[18F]fluoro-2-deoxy-D-glucose positron emission tomography (PET), magnetoencephalography (MEG), EEG-functional MRI (EEG-fMRI), high resolution-EEG (HR-EEG) and ictal single photon emission computed tomography (SPECT), have been proposed for the identification of the EZ. These procedures are expected to avoid or to guide invasive EEG monitoring, in patients with unrevealing MRI or with anatomic-electro-clinical discrepancies (An et al., 2013; Nakajima et al., 2016). However, only few papers have been assessed the multimodal functional investigations in detecting the EZ compared to the invasive procedures (see also Supplementary Files, Table A for main references). Moreover, no standardized protocols are available to evaluate the reliability of non-invasive procedures for the EZ identification, with large variations in the presurgical diagnostic workup among the different centers (Guerrini et al., 2013; Mouthaan et al., 2016).

Aim of the present study was to assess the usefulness of four NIFNTs (PET, MEG, EEG-fMRI, HR-EEG) to identify the EZ in patients with drug-resistant focal epilepsy candidate to Stereo-Electroencephalography (SEEG) with negative structural MRI. Results on the presumed EZ identification obtained from the different NIFNTs have been compared with data obtained from SEEG and with surgical or Radio-Frequency SEEG-Guided Thermocoagulation (RF-THC) (Cossu et al., 2014) outcome. Sensibility, specificity, positive predictive value (PPV), negative predictive value (NPV), and accuracy of each NIFN technique, and of their combinations, have been also evaluated, in order to verify the real diagnostic values in the workup of MRI-negative epileptic patients, candidate to surgery.

2. Methods

2.1. Patients recruitment and procedures

Forty-one were included in the study (25 M, mean age 32.2; SD \pm 8.8 years; range 18–47 years) and admitted to the following investigations: PET, MEG, EEG-fMRI and HR-EEG. However, not all patients underwent to all the NIFNTs, mainly because of organizational problems. Of the 41 patients enrolled, PET, MEG, EEG-fMRI and HR-EEG were performed in 40 (97.6%), 41 (100%), 27 (65.9%) and 35 (85.4%), respectively. In 3 patients (7.3%) only two NIFNTs were performed, while in 15 (36.6%) and 22 (53.7%), three and four evaluations were performed.

The patients were then admitted to SEEG investigation. SEEG was performed at the “Claudio Munari” Epilepsy Surgery Centre of the Niguarda Hospital (Milan, Italy), following the procedure that has been described previously (Cossu et al., 2005; Cardinale et al., 2013).

The patients' eligibility for epilepsy surgery and the surgical plan was decided after comprehensive discussion involving the referring epileptologists, neurosurgeons, and neuroradiologists, blind to NIFNTs results. Two patients were excluded from neurosurgery after this multidisciplinary discussion. In 33 of the 39 remaining patients, before SEEG electrodes removal, RF-THC was performed at the end of the monitoring period (Cossu et al., 2014). Thirty-two patients (including 26 who did not respond to RF-THC) were admitted to resective surgery; all the resections were performed for strictly therapeutic reasons and the extent of the excision was planned on the basis of anatomic-electro-clinical data and of the risk of postsurgical deficits. Fig. 1 summarizes the work-up of the study.

Neuropathological evaluations of the surgical specimens were performed according to the International League Against Epilepsy recommended procedure (Blumcke et al., 2016). Post-surgical outcome was evaluated in all the patients at 1 year after surgery, according with the Engel scale (Engel et al., 1993)

All the procedures and protocols have been approved by the Ethical Committees of institutions and performed after written informed consent by all of the patients.

2.2. Neuroimaging techniques

2.2.1. PET

PET were acquired, using a standard 11-min routine (1 min for transmission and 10 min for emission), using PET/CT Biograph equipment (Siemens, Erlangen, Germany). Thirty-five tomographic, attenuation-corrected brain sections were obtained (2.47-mm slice thickness) 40 min after an intravenous administration of 5 MBq/kg of ¹⁸F-DG. Reconstruction was performed with ordered subset expectation maximization algorithm (16 subsets and six iterations) with a matrix of 128 \times 128 \times 64 and 2.6 mm³ voxel size. PET were co-registered with individual 3D T1-weighted MRI images using a color-coded grading internally scaled to the occipital cortex or basal ganglia, and then visually inspected. Only regions with at least one well-defined hypometabolism were classified as positive. This qualitative approach was similar to that proposed by Rubi et al. (2011), with the difference that in our work the mild decreased uptakes were considered as negative. A nuclear medicine expert (ADS) identified the PET-presumed location of the EZ of each patient.

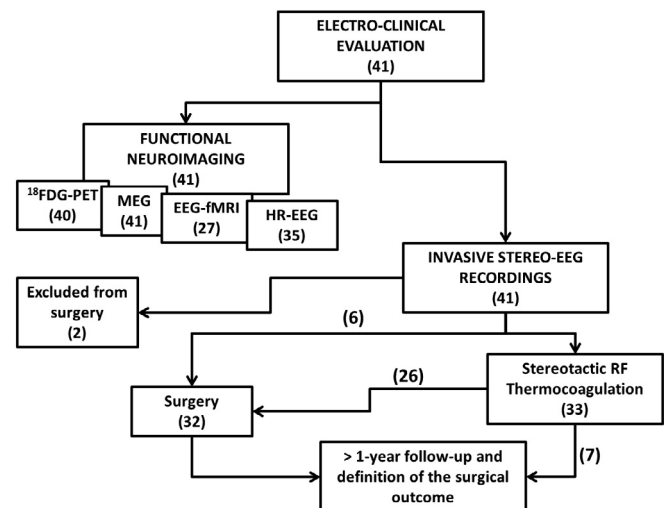


Fig. 1. Work up of the study. Legend: ¹⁸F-DG-PET = 2-[18F]fluoro-2-deoxy-D-glucose positron emission tomography; MEG = Magnetoencephalography; EEG-fMRI = Electroencephalography (EEG) - functional Magnetic Resonance Imaging; HR-EEG = High Resolution-EEG; RF = Radio-Frequency.

2.2.2. MEG

MEG data were acquired with a 306-channel whole head MEG system (Neuromag Triux, Megin Oy, Finland) at 1 kHz sampling frequency. To monitor and eventually correct the head position during the acquisition, five coils on the scalp together with three landmarks (nasion, right and left pre-auricularis points) were digitized before recording by a three dimensional digitizer (FASTRAK, Polhemus, Colchester, VT). Additional scalp points were also digitized for the co-registration with the patient's anatomical T1-weighted MRI. Data were pre-processed off-line with the temporally extended signal space separation method implemented in the Maxfilter 2.2 (Megin Oy, Finland) to suppress external interferences and correct for head movements (Taulu and Kajola, 2005; Guo et al., 2010), filtered at 0.1–100 Hz, and then visually inspected seeking for interictal epileptiform discharges (IEDs) (Enatsu et al., 2008). The source localization of IEDs was estimated at its peak by means of standardized low-resolution electromagnetic tomography (sLORETA) using a realistic individual boundary-element headmodel (BEM, Freesurfer, Martinos Center for Medical Imaging, Charlestown, MA, USA); threshold was set at 80%. A neurophysiologist (DRS) and a biomedical engineer (DD) collaborated to identify the MEG presumed location of the EZ of each patient.

2.2.3. EEG-fMRI

Functional imaging was performed on a 3 T MR scanner (Philips Healthcare BV, Best, The Netherlands); 800 functional volumes were acquired, corresponding to 2400 s, with patients at rest, while structural images were acquired by means of a volumetric T1-weighted sequence. Concurrent EEG and electrocardiographic recordings were acquired using a magnetic resonance-compatible device (SD MRI 32, Micromed, Mogliano Veneto, Italy) at a sampling rate of 1024 Hz, using a cap with 30 electrodes positioned according to the international 10–20 system. EEG signals were processed offline by means of the Brain Quick System Plus software (Micromed, Mogliano Veneto, Italy) in order to remove gradient and ballistocardiogram artifacts. Filtered EEG traces were visually reviewed to detect and classify IEDs and focal slow abnormalities into distinct types according to spatial distribution and morphology (SF, ES); then, their time onset was marked.

Functional imaging was pre-processed and analyzed using the SPM8 software (Wellcome Trust Centre for Neuroimaging, London, United Kingdom). Volumes were realigned and normalized into the Montreal Neurological Institute space. Gaussian smoothing was performed with a 7 mm Full Width at Half Maximum isotropic kernel. Each marked event of interest entered as regressor in the design matrix. In order to consider errors related to movement artifacts, six realignment regressors (three rotation and three translation parameters) were included in the design matrix.

The first-level individual analyses were made with General Linear Model (Friston et al., 1994). The effects were described on t-contrast maps using the family-wise error (FWE) correction for multiple comparisons with a voxel-level threshold of $p = 0.05$; when this approach did not reveal any significant difference, an uncorrected threshold of $p < 0.001$ was considered, with an additional extent threshold of 100 voxels. fMRI results were superimposed onto the individual co-registered T1-weighted images. Two biomedical engineers (FP and EV) and a neurophysiology technologist (ES) collaborated to identify the EEG-fMRI-presumed location of the EZ of each patient.

2.2.4. HR-EEG

HR-EEG recordings lasting about 60 minutes was acquired with a 256 electrodes equipment (Electrical Geodesic Inc., OR, United States of America) at a sampling rate of 1 kHz; the signal was band-pass filtered to 0.1–100 Hz. The signal was analyzed visually, in order to identify the presence of IEDs, with a procedure similar

to that used for MEG. Individual and/or averaged IEDs were localized with sLORETA methods using Curry 7 Neuroimaging suite (Compumedics Ltd., Australia); threshold was set at 80%. A realistic BEM model based on individual high-resolution 3D-T1 MRI was used to compute the forward solution using the Curry 7 software, coregistered through the digitized points reproducing the shape of the head of the subject. A neurophysiologist (LN) and a neurophysiology technologist (AR) collaborated to identify the HR-EEG-presumed location of the EZ of each patient.

2.3. Statistical analysis: Calculation of the diagnostic measures of neuroimaging techniques

2.3.1. Comparison between functional imaging techniques and SEEG results

For the 39 patients admitted to RF-THC and/or neurosurgery, the identification of EZ based on NIFNTs was compared with the EZ identified through the SEEG. For each NIFNTs, the concordance of the resulting solution with SEEG was classified by three expert clinical neurologists (FG, LT, RS) and a neurosurgeon (FC) as “concordant” (C) when the presumed EZ was localized in a single cortical gyrus included (even partially) in the surgical plan. Otherwise the solution was classified as non-concordant (NC). For cortical parcellation, the Desikan-Killiany atlas (Desikan et al., 2006) was used. The concordance or discordance between the NIFNTs results and SEEG was evaluated in the whole 39 patients and separately in the subgroup of 20 patients in whom the EZ, as indicated by SEEG, involved two or more lobes (multilobar = ML). The concordance or discordance between the NIFNTs results and SEEG were assessed for single (1), coupled (2), associated (3) and all (4) NIFNTs. When combinations of two or more NIFNTs together and SEEG results were compared, we considered the combination of NIFNTs as C with SEEG when all of the techniques included in the “combination” were concordant with SEEG; otherwise the combination of NIFNTs was considered NC.

2.3.2. Comparison between functional imaging techniques and postsurgical outcome: Calculation of diagnostic measures

Outcome at one year was taken as reference standard, discriminating between good (Engel's class I) and poor surgical outcome (Engel's classes II–IV).

NIFNTs results from each operated patient were classified with respect to concordance with SEEG and the outcome at 1-year after surgical resection or RF-THC as

- TRUE POSITIVE (TP): concordance between NIFNTs and SEEG with good outcome;
- FALSE POSITIVE (FP): concordance between NIFNTs and SEEG, with poor outcome;
- TRUE NEGATIVE (TN): discordance between NIFNTs or between NIFNTs and SEEG with poor outcome;
- FALSE NEGATIVE (FN): discordance among NIFNTs or between NIFNTs and SEEG with good outcome.

Then, the following diagnostic measures were calculated:

- SENSITIVITY = $TP / (TP + FN)$;
- SPECIFICITY = $TN / (TN + FP)$;
- PPV = $TP / (TP + FP)$;
- NPV = $TN / (TN + FN)$;
- Accuracy = $(TP + TN) / (TP + FP + TN + FN)$;

Sensitivity, specificity, PPV, NPV and accuracy were assessed for single (1), coupled (2), associated (3) and all (4) NIFNTs with 95% confidence limits, as suggested by the STARD initiative (Bossuyt et al., 2003).

3. Results

3.1. Patients summary

Table 1 summarizes the patients' data in the whole population. In the 39 patients admitted to RF-THC and/or neurosurgery, EZ was localized, by SEEG, in the left hemisphere in 21 patients and in the right one in 18 patients. EZ involved the temporal lobe (including amygdala, hippocampus and insula) in 29 patients, the frontal lobe in 15 patients, and the parietal, occipital and central (including precentral and postcentral gyri) lobes in 8, 7 and 4 patients, respectively.

In 19 patients (48,7%) EZ involved only one lobe; in 10 of them, the EZ was identified inside the temporal lobe, and in 9 in extra-temporal regions; in the remaining 20 patients (51,3%) EZ involved more than one lobe (ML subgroup; 10 M, mean age 34.8 ± 9.0 yrs., range 16–46 yrs).

RF-THC was performed in 33 patients; however, since in 26 patients this procedure failed to control seizures, a resective surgery was subsequently performed. A total of 32 patients

underwent resective surgery, thus allowing neuropathological diagnosis and revealing that 22 patients (69%) showed only reactive gliosis on the resected specimen (considered as cryptogenic); a Focal Cortical Dysplasia type I or type II was diagnosed in 7 (22%) and in 3 (9%), respectively (see also Table 1).

After at least 1-year of follow-up, 27 patients (69.2%) were in Engel Class I, while 12 (31,8%) in Class II-IV: 4 patients in Class II, 4 in Class III and 4 in Class IV, respectively.

In the ML subgroup, 9 patients (45,0%) were in Engel Class I and 11 (55%) in Class II-IV: 3 in Class II, 4 in Class III and 4 in Class IV, respectively.

3.2. Functional imaging techniques

Fig. 2 shows an example in which solutions from NIFNTs and SEEG are embedded all together in a 3D reconstruction of patient's brain (patient #2).

Table 2 summarizes the concordance between NIFNTs and SEEG and the diagnostic yield (i.e. sensitivity, specificity and accuracy) of

Table 1
Summary of clinical, neurophysiological, neuropathological and functional data of the patients.

Patients	Gender	Age (y)	Disease duration (y)	EZ localization (SEEG)	RF-THC	Surgery	Neuro pathology	outcome (Engel' class)	Concordance NIFNTs-SEEG			
									PET	MEG	EEG-fMRI	HR-EEG
#1	M	22	3	Left F	X	X	FCD Ia	I	NC	C	***	C
#2	M	27	8	Right F + T + I	***	X	gliosis	I	C	C	C	C
#3	M	25	20	Left T + I	X	X	gliosis	I	C	NC	NC	NC
#4	F	30	14	Right T	X	X	gliosis	I	C	C	C	C
#5	M	20	19	Right F	***	X	gliosis	I	NC	C	***	NC
#6	M	43	28	Left F + T	X	X	gliosis + HS	I	C	C	C	C
#7	M	46	16	Left F + T	X	***	***	III	C	C	***	***
#8	F	27	10	Left T	X	X	gliosis	I	NC	NC	NC	C
#9	F	36	28	Left T	X	***	***	I	C	NC	NC	***
#10	M	40	24	Left F	X	***	***	I	C	NC	NC	C
#11	F	31	19	Left T + I + P	X	X	gliosis	IV	NC	NC	NC	C
#12	F	35	31	Right C + T	X	X	FCD Ib	II	***	C	C	NC
#13	M	43	25	Right F + T	X	X	FCD Ib	III	NC	NC	***	C
#14	M	34	13	Right T + P + O	X	***	***	IV	C	C	***	C
#15	F	22	12	Left P + I	X	X	FCD IIa	II	NC	NC	NC	C
#16	M	19	9	Right O	X	***	***	I	C	C	NC	NC
#17	F	20	4	Left T	X	X	gliosis	I	C	NC	C	NC
#18	F	24	22	Right C + P	***	X	FCD IIa	I	C	C	***	***
#19	M	24	7	Right F	X	X	FCD Ia	I	C	NC	C	NC
#20	F	44	25	Left F	X	X	gliosis	I	NC	C	C	C
#21	M	39	19	Left F	X	X	gliosis	I	C	NC	***	NC
#22	F	31	30	Right T	X	X	gliosis + HS	I	C	NC	NC	***
#23	F	40	25	Left T + O	***	X	gliosis	I	C	C	***	***
#24	M	29	19	Left P	X	X	gliosis	I	C	NC	C	***
#25	M	35	6	Right T	X	X	gliosis	I	NC	NC	NC	C
#26	M	34	7	Right T	***	X	gliosis	I	NC	C	***	C
#27	F	42	24	Right T + O	X	X	FCD Ia	I	C	C	***	NC
#28	M	16	16	Left T + P + O	X	X	gliosis	I	C	C	C	C
#29	F	38	18	Right F + C + T	X	X	gliosis	IV	C	C	NC	NC
#30	F	26	8	Left F + T + I	X	***	***	IV	C	C	***	NC
#31	M	45	28	Left T	X	X	gliosis	II	C	C	NC	NC
#32	M	18	7	Left F	***	X	gliosis	I	C	C	C	C
#33	M	29	5	Right T	X	X	FCD Ia	I	C	C	C	C
#34	F	40	34	Right F + T	X	X	FCD IIb	I	C	C	C	C
#35	M	45	29	Right T + P	X	***	***	III	C	NC	***	C
#36	M	22	7	Right T + O	X	X	gliosis	I	C	C	NC	C
#37	F	37	28	Left C + P + T	X	X	gliosis	III	C	C	NC	C
#38	M	40	13	Left F + T + I	X	X	gliosis	II	C	C	NC	C
#39	M	44	22	Left T + O	X	X	FCD Ib	I	NC	C	***	C
#40	M	33	12	Unknown	X	***	***	NE	NE	NE	***	NE
#41	F	26	6	Unknown	***	***	***	NE	NE	NE	NE	NE

Legend: In the first line, EZ = Epileptogenic Zone, SEEG = Stereo-Electroencephalography (EEG), RF-THC = Radio-Frequency SEEG-Guided Thermocoagulation, NIFNTs = Non-Invasive Functional Neuroimaging techniques, PET = 2-[18F]fluoro-2-deoxy-D-glucose positron emission tomography, MEG = magnetoencephalography, EEG-fMRI = EEG-functional Magnetic Resonance Imaging, HR-EEG = High resolution-EEG; in "EZ localization" column, C = central (precentral and postcentral gyri), F = frontal lobe, I = insula, n. a. = not available, O = occipital lobe, P = parietal lobe, T = temporal lobe; in "neuropathology" column: FCD = focal cortical dysplasia, HS = hippocampal sclerosis; in "surgery", "PET", "MEG" "EEG-fMRI" and "HR-EEG" columns: X = performed; ***=not performed; in the "concordance NIFNT-SEEG" column: C = concordant; NC = non-concordant; NE = non-evaluable.

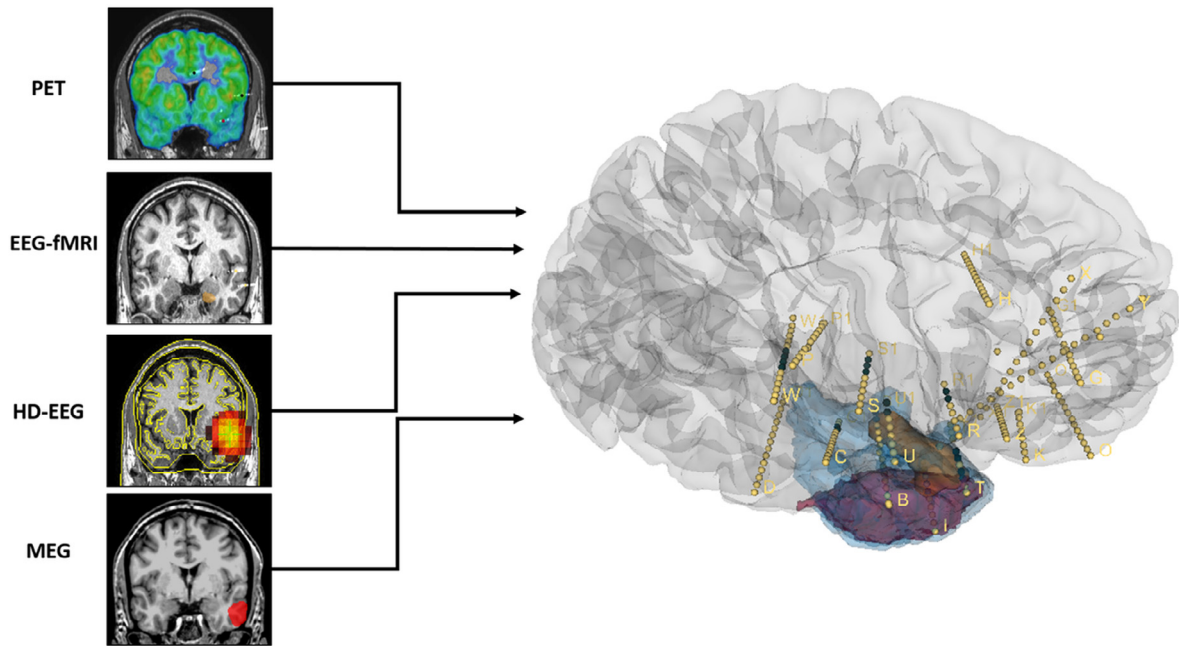


Fig. 2. Example of multimodal integration of functional techniques. A multimodal integration is shown (patient #2). Epileptogenic Zone obtained from Magnetoencephalography (MEG, in red) and electroencephalography (EEG)-functional Magnetic Resonance Imaging (MRI) (orange) are embedded into the subject's volumetric 3D MRI together with Stereo-EEG electrodes coordinates (yellow). Positron Emission Tomography (PET) and High Resolution-EEG solutions overlapped for the most the MEG solution and they were not included for an easier graphical interpretation of the figure. The resected area is shown in blue and was obtained from the post-operative MRI. (For interpretation of the references to colour in this figure legend, the reader is referred to the web version of this article.)

single techniques and all of them considered together, both for all the patients and the ML subgroup.

Complete data with all the diagnostic measures and confidence limits are detailed in [Supplementary Files, Table B](#) (all operated patients) and Table C (ML subgroup).

[Fig. 3](#) shows a comparison of the concordance between NIFNTs and SEEG with the accuracy when one, two, three or all the NIFNTs were used, in both all patients and ML subgroup.

3.2.1. Comparison between functional imaging techniques and SEEG results

3.2.1.1. All the patients. PET MEG and HR-EEG reached a high concordance with SEEG results (about 70%), with the best concordance obtained by PET (73.7%), while EEG-fMRI showed a concordance of 46.2% with SEEG. When two or more NIFNTs were considered together, concordance with SEEG decreased, achieving about 40–45% when two techniques were combined (best concordance for PET-MEG combination, 50.0%), about 30–35% when three techniques were combined (best concordance for MEG-EEG-fMRI-HR-EEG, 34.8%) and 31.8% when all NIFNTs were considered together.

3.2.1.2. ML subgroup. In the ML subgroup the trends remained the same, with improvements in concordance for PET, MEG and HR-EEG when considered alone (best concordance for MEG, 80.0%), but not for EEG-fMRI (45.5%). Again, when combined NIFNTs were considered, concordance with SEEG progressively decreased, up to only 40.0% of all techniques considered together.

3.2.2. Comparison between functional imaging techniques and postsurgical outcome: The diagnostic yield

3.2.2.1. All the patients. PET, MEG, and HR-EEG had higher sensitivity (range 64.3–78.6%) and PPV (68.2–75.9%) than specificity (30.0–36.4%) and NPV (27.3–36.4%), whereas EEG-fMRI showed a lower sensitivity (55.0–60.0%), higher specificity (83.3%) and PPV (91.7–92.3%) and similar NPV (35.7–38.4%) than other techniques. When concordance among combinations of two or more NIFNTs and

SEEG results were considered together, sensitivity decreased, while specificity and PPV increased, NPV was similar with respect to the values obtained from single techniques. By considering two coupled NIFNTs, MEG/HR-EEG had the best sensitivity (47.8–65.2%) and the best NPV (36.8–46.7%), while PET/EEG-fMRI had the best specificity and the best PPV (reaching 100% for both). By considering the combination of three NIFNTs techniques; the best accuracies was reached when MEG, EEG-fMRI, and HR-EEG were considered together (60.9–65.2%).

3.2.2.2. ML subgroup. In the ML subgroup of patients, both the diagnostic values of single and combined NIFNTs increased. MEG was always concordant with SEEG in all of the seizure-free patients after surgery (i.e., 100% sensitivity), while EEG-fMRI reached the highest specificity (i.e. 83.3%). Among paired techniques MEG/HR-EEG and PET/MEG showed the best sensitivity (85.7–88.9%), while PET/EEG-fMRI and EEG-fMRI/HR-EEG the best specificity and the best PPV (reaching 100% for both); NPV had similar values for all the combination of techniques (best values 87.5% for MEG/HR-EEG). Accuracy achieved high values, until 90.9% for EEG-fMRI/HR-EEG. When results of three techniques, including EEG-fMRI, or of all the four techniques (10 patients) were considered together, NIFNTs achieved 100% for specificity and PPV, and very high values for sensitivity (80.0%) and NPV (83.3–85.7%); accuracy had high values, reached 90.9% for PET/MEG/EEG-fMRI or MEG/EEG-fMRI/HR-EEG and 83.3% when all the techniques were considered together.

3.3. Note on patients excluded from RF-THC and/or neurosurgery

Two patients (i.e. #40 and #41) were excluded from neurosurgery; hence, NIFNTs concordance with respect to the EZ localization and the diagnostic measures with respect to the surgical outcome could not be calculated. For both patients, NIFNTs results were discordant with each other.

Table 2
Concordance with SEEG and diagnostic measures with respect to outcome of NIFNs – All operated patients/ML subgroup.

Technique	Number of patients	Concordance with SEEG %	Diagnostic Measures		
			Sensitivity % (IC %)	Specificity % (IC %)	Accuracy % (IC %)
All operated patients					
PET	38	73.7	75.0 (59.0–91.0)	30.0 (1.0–91.0)	63.2 (47.8–78.5)
MEG	39	64.1	64.3 (46.5–82.0)	36.4 (7.9–64.8)	56.4 (40.8–72.0)
EEG-fMRI	26	46.2	55.0 (33.2–76.8)	83.3 (53.5–100)	61.5 (42.8–80.2)
HR-EEG	33	66.7	65.2 (45.7–84.7)	30.0 (1.6–58.4)	54.6 (37.6–71.5)
All techniques	22	31.8	41.4 (17.8–64.6)	100 (46.3–100)	54.5 (35.7)
Multilobar subgroup					
PET	19	78.9	88.9 (68.4–100)	30.0 (1.6–58.4)	57.9 (35.7–80.1)
MEG	20	80.0	100 (62.9–100)	36.4 (7.9–64.8)	65.0 (44.1–85.9)
EEG-fMRI	11	45.5	80.0 (44.9–100)	83.3 (53.5–100)	81.8 (59.0–100)
HR-EEG	17	70.6	85.7 (59.8–100)	40.0 (9.6–70.4)	58.9 (35.4–82.2)
All techniques	10	40.0	80.0 (44.9–100)	100 (46.3–100)	83.3 (71.4–100)

Legend: SEEG = Stereo-Electroencephalography (EEG), NIFNs = Non-Invasive Functional Neuroimaging techniques, PET = 2-[18F]fluoro-2-deoxy-D-glucose positron emission tomography, MEG = magnetoencephalography, EEG-fMRI = EEG-functional Magnetic Resonance Imaging, HR-EEG = High resolution-EEG; IC = Interval Confidence (at 95%). Concordance with SEEG, sensitivity, specificity, and accuracy are expressed in percentage with IC indicated in brackets.

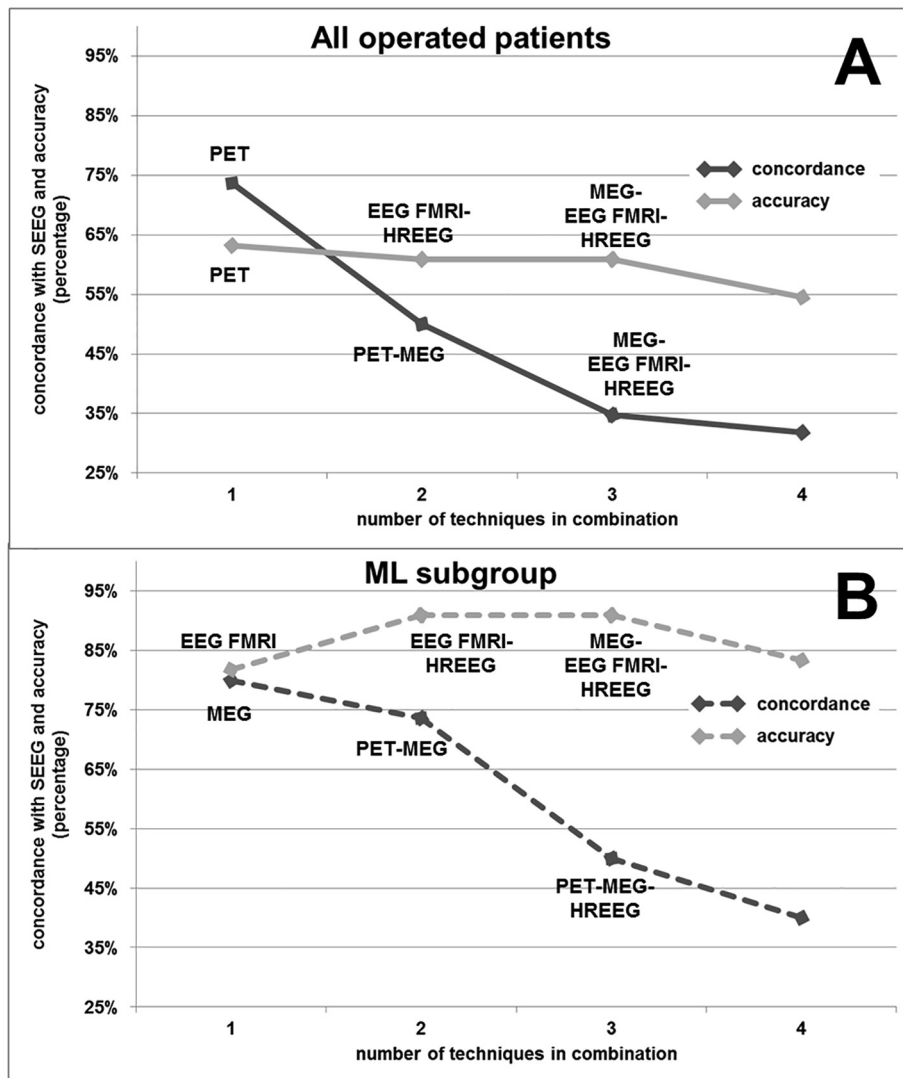


Fig. 3. Higher concordance and accuracy when 1,2,3,4 NIFNTs were used (all patients operated and ML subgroup). Dark lines represent higher concordance with Stereo-Electroencephalography, while grey lines higher accuracy with respect to the outcome between single techniques or combinations of them when one, two or three NIFNTs were used in all patients (A) and in ML subgroup (B). The technique (or the combination of the techniques) with higher concordance/accuracy are indicated over the lines. When considering up to three techniques, in ML subgroup accuracy with respect to outcomes increases while concordance with SEEG decreases; this effect is due to the increase of the specificity. Legend: NIFNTs = Non-invasive functional neuroimaging techniques; ML = Multilobar; PET = 2-[18F]fluoro-2-deoxy-D-glucose positron emission tomography; MEG = Magnetoencephalography; EEG-fMRI = Electroencephalography (EEG) - functional Magnetic Resonance Imaging; HR-EEG = High Resolution-EEG.

Patient #40 underwent PET, MEG and HR-EEG. EZ was identified in the right parieto-occipital, in the right frontal and in right temporal lobes with PET, MEG and HR-EEG results, respectively.

Patient #41 underwent all NIFNTs. EZ was identified in an extended left fronto-temporo-insular area with PET and in the left temporal lobe with HR-EEG, and she resulted as multifocal with MEG, while EEG-fMRI was not able to identify any EZ.

4. Discussion

In the field of epilepsy surgery, the best prognostic factor of the pre-surgical evaluation is the precise identification of the EZ. When discrepancies between non-invasive electro-clinical and imaging data are present, and particularly in patients with negative MRI, invasive monitoring is often required. In this contest, the use of NIFNTs seems promising since they may yield complementary information (Pittau et al., 2014), potentially useful to prevent or refine invasive recording.

The aim of this study was to assess the diagnostic value of four different NIFNTs in the diagnostic workup of MRI-negative epileptic patients, candidate to surgery. The diagnostic value was evaluated in a “two-steps analysis”, by first measuring the concordance of NIFNTs with SEEG, and then by comparing the results with the postoperative outcome, being the validation proven by a co-localization of the EZ within the resection and the patient seizure-free after surgery (Pittau et al., 2014). Thus, to obtain an objective method, we classified the patients with respect to NIFNTs-SEEG concordance and to postsurgical outcome (one year of follow-up).

Authors (Koessler et al., 2010) reported a SEEG versus HR-EEG agreement ranging from 50% to 90%, depending on the different source localization method used. In a very large cohort of 455 drug-resistant epileptic patients, Stefan et al., 2003, indicated an average sensitivity for MEG of 70%, while Nissen et al., 2016, reported a good identification of the EZ by MEG in 68% of the patients. Jung et al., 2013, showed a mean sensitivity of 81% for MEG in a group of MRI-negative patients with focal epilepsy. Centeno et al., 2017, reported a good localization of EZ by EEG-fMRI in 57.9% of children submitted to surgery.

In a recent, large prospective study (Duez et al., 2019), the electromagnetic source imaging (i.e. source imaging resulted from MEG and HR-EEG combined) showed accuracy ranging 44–57%; in this study, the use of the solution proposed by the electromagnetic source imaging contributed to modify the management of the surgical plan in 34% of the patients. Overall, a systematic review of the E-PILEPSY consortium including 11 studies, estimated sensitivity and specificity 82% (95% CI: 75–88%) and 53% (95% CI: 37–68%), respectively, for both MEG and HR-EEG, with no statistical difference between them (Mouthaan et al., 2019).

In a retrospective study on MRI-negative/PET-positive temporal lobe epilepsies, Feng et al., 2014, reported 84.2% of seizure-free patients after resective surgery and Rathore et al., 2014, reported that PET showed unifocal hypometabolism in 50.5% and bilateral hypometabolism in 12% of their cohort. Knowlton et al. (2008a, b), reported MEG and PET sensitivity ranging from 58 to 64% and from 22 to 40%, respectively, while specificity ranged from 79 to 88% for MEG and from 53 to 63% for PET.

In our study, when the whole cohort of patients underwent RF-THC and/or neurosurgery is considered, each technique had accuracy values of about 60%; having PET, MEG and HR-EEG higher sensitivity, and EEG-fMRI higher specificity. When the combination of two or more NIFNTs was considered, we did not find any substantial improvement. In fact, the increased specificity (up to 100% when three techniques, including EEG-fMRI, or four techniques were considered) was paralleled by a decreased sensitivity (with

accuracy reaching its highest value when MEG/EEG-fMRI/HR-EEG were combined together). This result is in agreement with previous data reported by Knowlton et al. (2008a,b), about the combination of MEG/PET.

The results obtained in our study with each technique is comparable with those of literature, although little differences should be accounted, due to the challenging group of patients enrolled for the study (i.e. MRI-negative patients) and to the stringent criteria adopted for the definition of concordance between NIFNTs and SEEG results, because we applied a cortical parcellation atlas that provides 35 areas based on gyral morphology (Desikan et al., 2006) to define our ROIs. Furthermore, for the localization of epileptic activity, we considered only IEDs (for EEG-fMRI, HR-EEG and MEG) and focal non-epileptic abnormalities (slow activity for EEG-fMRI), although being the invasive monitoring principally based on ictal data. It has been already reported that IEDs represent a valid surrogate for the EZ localization (Hufnagel et al., 2000) since IEDs-based analysis agree with information derived from intracerebral recordings (see Pittau et al., 2014, for review). Nevertheless, the possibility that ictal and interictal sources are not coincident and that would in part explain in some cases the differences between SEEG and NIFNTs. The literature agrees to consider functional imaging techniques as “optional” and to suggest their execution before intracranial exploration, as in the pathways of assessment for epilepsy surgery proposed by Duncan et al. (2016).

Our data suggest that the usefulness of NIFNTs also depends on the subgroup of patients to be studied: in the whole sample of patients, the use of NIFNTs alone appeared fruitless, for the poor diagnostic yield (accuracy ranging about 50–65%), also considering the high costs of each techniques, rendering the invasive explorations mandatory. On the other hand, when only the ML subgroup was considered, the NIFNTs showed encouraging results. We can hypothesize that some patients may have a wide epileptogenic network, revealed by NIFNTs, but “underestimated” by the SEEG and thus not included in the surgical plan. Furthermore, in an “unexpected” way, our data show that, considering an increasing number of techniques combined together, the concordance between the result of the NIFNTs techniques and the SEEG decreases, but increases their diagnostic accuracy (with respect to the surgical outcome); this trend is particularly marked in the ML subgroup of patients. In part this result depends on the study design, because we considered the combination of NIFNTs as C with SEEG only if all of them were C with SEEG. However, this does not explain the parallel increase in accuracy, which appears due to the increase in specificity and NPV that occurs when three or four NIFNTs are taken into consideration. When results from multiple techniques were combined together, specificity and PPV tended to rise, while sensitivity and NPV remain similar, thus increasing the accuracy. The best results were achieved when at least three techniques, including EEG-fMRI, were considered together, suggesting an improvement of the diagnostic value, namely in predicting predict an unfavorable surgical outcome (high NPV), suggesting a reevaluation of the surgical plan or prevent inappropriate surgery.

The results of NIFNTs in two patients excluded from surgery, due to the failure to define EZ, further support this hypothesis. Obviously, for these patients the diagnostic yield of NIFNTs could not be calculated with respect to EZ localization and to post-surgical outcome. However it is remarkable to note that in both patients the NIFNTs were all non-concordant, endorsing the hypothesis that different results in the localization of the EZ with NIFNTs could help in preventing inappropriate surgery.

Our results underlined that at least three NIFNTs should be included in the pre-surgical workup, because it greatly increased accuracy, namely in a subgroup of patients with “extended” EZ: all the performed techniques had high sensitivity and low

specificity, with the exception of the EEG-fMRI, which conversely showed a very high specificity; hence it should be included in the work-up. MEG and HR-EEG had the greater PPV either with respect to the outcome, considered alone or in combination in ML subgroup of patient. Consequently, MEG should be included, considering HR-EEG as an effective alternative, because organizational and economic constraints may prevent the widespread use of MEG. PET provides complementary information with respect to other NIFNTs (i.e., metabolic abnormalities) and must be included too.

These results seem promising, although they must be confirmed by further prospective studies on larger cohort and the cost/benefit analysis to determine which technique(s) is (are) necessary or sufficient to give the best result should be evaluated, without forgetting that the inclusion of these techniques represent an organizational problem.

Acknowledgements and funding sources

We want to thank Cristina Popescu and Claudio Rossetti (Nuclear Medicine, Niguarda Hospital, Milan, Italy) for their contribution and for their time spent for analysis. The authors disclosed receipt of the following financial support for the research, authorship, and/or publication of this article: DESIRE (Strategies for Innovative Research to Improve Diagnosis, Prevention and Treatment in children with difficult to treat epilepsy), a FP7 funded project (Grant Agreement no: 602531), from European Commission, the grants RF-2011-02350578 and RF-2010-2319316 from Italian Ministry of Health.

Declaration of Competing Interest

None of the authors has any conflict of interest to disclose. We confirm that we have read the journal's position on the issues involved in ethical publication, and affirm that this report is consistent with those guidelines.

Appendix A. Supplementary material

Supplementary data to this article can be found online at <https://doi.org/10.1016/j.clinph.2020.05.015>.

References

- An D, Fahoum F, Hall J, Olivier A, Gotman J, Dubeau F. Electroencephalography/functional magnetic resonance imaging responses help predict surgical outcome in focal epilepsy. *Epilepsia* 2013;54:2184–94. <https://doi.org/10.1111/epi.12434>.
- Bien CG, Szinay M, Wagner J, Clusmann H, Becker AJ, Urbach H. Characteristics and surgical outcomes of patients with refractory magnetic resonance imaging-negative epilepsies. *Arch Neurol* 2009;66:1491–9. <https://doi.org/10.1001/archneurol.2009.283>.
- Blümcke I, Aronica E, Miyata H, Sarnat HB, Thom M, Roessler K, et al. International recommendation for a comprehensive neuropathologic workup of epilepsy surgery brain tissue: A consensus Task Force report from the ILAE Commission on Diagnostic Methods. *Epilepsia* 2016;57:348–58. <https://doi.org/10.1111/epi.13319>.
- Bossuyt PM, Reitsma JB, Bruns DE, Gatsonis CA, Glasziou PP, Irwig LM, et al. Toward complete and accurate reporting of studies of diagnostic accuracy: The STARD initiative. *Am J Clin Pathol* 2003;119:18–22. <https://doi.org/10.1309/8EXCCM6YR1THUBAE>.
- Burneo JG, Steven DA, McLachlan RS, Parrent AG. Morbidity associated with the use of intracranial electrodes for epilepsy surgery. *Can J Neurol Sci* 2006;33:223–7. <https://doi.org/10.1017/S0317167100005023>.
- Cardinale F, Cossu M, Castana L, Casaceli G, Schariati MP, Miserocchi A, et al. Stereoelectroencephalography: Surgical methodology, safety, and stereotactic application accuracy in 500 procedures. *Neurosurgery* 2013;72:353–66. <https://doi.org/10.1227/NEU.0b013e31827d1161>.
- Centeno M, Tierney TM, Perani S, Shamshiri EA, St Pier K, Wilkinson C, et al. Combined electroencephalography–functional magnetic resonance imaging and electrical source imaging improves localization of pediatric focal epilepsy. *Ann Neurol* 2017;82:278–87. <https://doi.org/10.1002/ana.25003>.
- Cossu M, Cardinale F, Castana L, Citterio A, Francione S, Tassi L, et al. Stereoelectroencephalography in the presurgical evaluation of focal epilepsy: a retrospective analysis of 215 procedures. *Neurosurgery* 2005;57:706–18. <https://doi.org/10.1093/neurosurg/57.4.706>.
- Cossu M, Fuschillo D, Cardinale F, Castana L, Francione S, Nobili L, et al. Stereo-EEG-guided radio-frequency thermocoagulations of epileptogenic grey-matter nodular heterotopy. *J Neurol Neurosurg Psychiatry* 2014;85:611–7. <https://doi.org/10.1136/jnnp-2013-305514>.
- Desikan RS, Ségonne F, Fischl B, Quinn BT, Dickerson BC, Blacker D, et al. An automated labeling system for subdividing the human cerebral cortex on MRI scans into gyral based regions of interest. *Neuroimage* 2006;31:968–80. <https://doi.org/10.1016/j.neuroimage.2006.01.021>.
- Duez L, Tankisi H, Hansen PO, Sidenius P, Sabers A, Pinborg LH, et al. Electromagnetic source imaging in presurgical workup of patients with epilepsy: A prospective study. *Neurology* 2019;92:e576–86. <https://doi.org/10.1212/WNL.00000000000006877>.
- Duncan JS, Winston GP, Koepp MJ, Ourselin S. Brain imaging in the assessment for epilepsy surgery. *Lancet Neurol* 2016;15:420–33. [https://doi.org/10.1016/S1474-4422\(15\)00383-X](https://doi.org/10.1016/S1474-4422(15)00383-X).
- Enatsu R, Mikuni N, Usui K, Matsubayashi J, Taki J, Begum T, et al. Usefulness of MEG magnetometer for spike detection in patients with mesial temporal epileptic focus. *Neuroimage* 2008;41:1206–19. <https://doi.org/10.1016/j.neuroimage.2008.03.038>.
- Engel Jr., P.C. Van Ness, T.B. Rasmussen, L.M. Ojemann. Surgical treatment of the epilepsies outcome with respect to epileptic seizures. Engel Jr. (Ed.), *Surgical Treatment of the Epilepsies* (second ed.), Raven Press, New York (1993), pp. 609–621.
- Feng R, Hu J, Pan L, Shi J, Qiu C, Lang L, et al. Surgical treatment of MRI-negative temporal lobe epilepsy based on PET: A retrospective cohort study. *Stereotact Funct Neurosurg* 2014;92:354–9. <https://doi.org/10.1159/000365575>.
- Friston KJ, Holmes AP, Worsley KJ, Poline J-P, Frith CD, Frackowiak RSJ. Statistical parametric maps in functional imaging: A general linear approach. *Hum Brain Mapp* 1994;2:189–210. <https://doi.org/10.1002/hbm.460020402>.
- Guerrini R, Scerrati M, Rubboli G, Esposito V, Colicchio G, Cossu M, et al. Overview of presurgical assessment and surgical treatment of epilepsy from the Italian League Against Epilepsy. *Epilepsia* 2013;7(Suppl):35–48. <https://doi.org/10.1111/epi.12308>.
- Guo C, Li X, Taulu S, Wang W, Weber DJ. Real-time robust signal space separation for magnetoencephalography. *IEEE Trans Biomed Eng* 2010;57:1856–66. <https://doi.org/10.1109/TBME.2010.2043358>.
- Hufnagel A, Dümpelmann M, Zentner J, Schijns O, Elger CE. Clinical relevance of quantified intracranial interictal spike activity in presurgical evaluation of epilepsy. *Epilepsia* 2000;41:467–78. <https://doi.org/10.1111/j.1528-1157.2000.tb00191.x>.
- Jung J, Bouet R, Delpuech C, Ryvlin P, Isnard J, Guenet M, et al. The value of magnetoencephalography for seizure-onset zone localization in magnetic resonance imaging-negative partial epilepsy. *Brain* 2013;136:3176–86. <https://doi.org/10.1093/brain/awt213>.
- Knowlton RC, Elgavish RA, Limdi N, Bartolucci A, Ojha B, Blount J, et al. Functional imaging: I. Relative predictive value of intracranial electroencephalography. *Ann Neurol* 2008;64:25–34. <https://doi.org/10.1002/ana.21389>.
- Knowlton RC, Elgavish RA, Bartolucci A, Ojha B, Limdi N, Blount J, et al. Functional imaging: II. Prediction of epilepsy surgery outcome. *Ann Neurol* 2008;64:35–41. <https://doi.org/10.1002/ana.21419>.
- Koessler L, Benar C, Maillard L, Badier JM, Vignal JP, Bartolomei F, et al. Source localization of ictal epileptic activity investigated by high resolution EEG and validated by SEEG. *Neuroimage* 2010;51:642–53. <https://doi.org/10.1016/j.neuroimage.2010.02.067>.
- Marras CE, Canevini MP, Colicchio G, Guerrini R, Rubboli G, Scerrati M, et al. Health Technology Assessment report on the presurgical evaluation and surgical treatment of drug-resistant epilepsy. *Epilepsia* 2013;54:49–58. <https://doi.org/10.1111/epi.12309>.
- Mouthaan BE, Rados M, Barsi P, Boon P, Carmichael DW, Carrette E, et al. Current use of imaging and electromagnetic source localization procedures in epilepsy surgery centers across Europe. *Epilepsia* 2016;57:770–6. <https://doi.org/10.1111/epi.13347>.
- Mouthaan BE, Rados M, Boon P, Carrette E, Diehl B, Jung J, et al. E-PILEPSY consortium. Diagnostic accuracy of interictal source imaging in presurgical epilepsy evaluation: A systematic review from the E-PILEPSY consortium. *Clin Neurophysiol* 2019;130:845–55. <https://doi.org/10.1016/j.clinph.2018.12.016>.
- Nakajima M, Widjaja E, Baba S, Sato Y, Yoshida R, Tabei M, et al. Remote MEG dipoles in focal cortical dysplasia at bottom of sulcus. *Epilepsia* 2016;57:1169–78. <https://doi.org/10.1111/epi.13399>.
- Nissen IA, Stam CJ, Citroen J, Reijneveld JC, Hillebrand A. Preoperative evaluation using magnetoencephalography: Experience in 382 epilepsy patients. *Epilepsy Res* 2016;124:23–33. <https://doi.org/10.1016/j.epilepsyres.2016.05.002>.
- Picot MC, Jaussent A, Neveu D, Kahane P, Crespel A, Gelisse P, et al. Cost-effectiveness analysis of epilepsy surgery in a controlled cohort of adult patients with intractable partial epilepsy: A 5-year follow-up study. *Epilepsia* 2016;57:1669–79. <https://doi.org/10.1111/epi.13492>.
- Pittau F, Grouiller F, Spinelli L, Seeck M, Michel CM, Vuillimoz S. The role of functional neuroimaging in pre-surgical epilepsy evaluation. *Front Neurol* 2014;5:31. <https://doi.org/10.3389/fneur.2014.00031>.
- Rathore C, Dickson JC, Teotónio R, Ell P, Duncan JS. The utility of 18F-fluorodeoxyglucose PET (FDG PET) in epilepsy surgery. *Epilepsy Res* 2014;108:1306–14. <https://doi.org/10.1016/j.epilepsyres.2014.06.012>.

- Rubí S, Setoain X, Donaire A, Bargalló N, Sanmartí F, Carreño M, et al. Validation of FDG-PET/MRI coregistration in nonlesional refractory childhood epilepsy. *Epilepsia* 2011;52:2216–24. <https://doi.org/10.1111/j.1528-1167.2011.03295.x>.
- Stefan H, Hummel C, Scheler G, Genow A, Druschky K, Tilz C, et al. Magnetic brain source imaging of focal epileptic activity: A synopsis of 455 cases. *Brain* 2003;126:2396–405. <https://doi.org/10.1093/brain/awg239>.
- Tanriverdi T, Ajlan A, Poulin N, Olivier A. Morbidity in epilepsy surgery: an experience based on 2449 epilepsy surgery procedures from a single institution. *J Neurosurg* 2009;110:1111–23. <https://doi.org/10.3171/2009.8.JNS08338>.
- Taulu S, Kajola M. Presentation of electromagnetic multichannel data: The signal space separation method. *J Appl Phys* 2005;97:12905–10. <https://doi.org/10.1063/1.1935742>.
- Télez-Zenteno JF, Dhar R, Wiebe S. Long-term seizure outcomes following epilepsy surgery: A systematic review and meta-analysis. *Brain* 2005;128:1188–98. <https://doi.org/10.1093/brain/awh449>.
- Wellmer J, Quesada CM, Rothe L, Elger CE, Bien CG, Urbach H. Proposal for a magnetic resonance imaging protocol for the detection of epileptogenic lesions at early outpatient stages. *Epilepsia* 2013;54:1977–87. <https://doi.org/10.1111/epi.12375>.